BULLETIN OF THE POLISH ACADEMY OF SCIENCES
TECHNICAL SCIENCES, Vol. 66, No. 5, 2018
DOI: 10.24425/124280

Application of novel discrete differential operator of periodic function to study electromechanical interactions

T.J. SOBCZYK[1]* and M. RADZIK[2]

[1]Cracow University of Technology, Institute on Electromechanical Energy Conversion, Warszawska Str. 24, 31-155 Cracow, Poland
[2]Technical Institute, State Higher Vocational School in Nowy Sącz, Zamenhofa 1a, 33-300 Nowy Sącz, Poland

Abstract. This paper investigates an algorithm for finding steady-states in electromechanical systems for the cases of their periodic nature. The algorithm enables to specify the steady-state solution identified directly in time domain. The basis for such an algorithm is a discrete differential operator that specifies the values of the first derivative of the periodic function in the selected set of points on the basis of the values of that function in the same set of points. It creates algebraic equations describing the steady-state solution for the nonlinear differential equations describing electromechanical systems. In this paper, the direct time-domain approach is tested for the simple converter considering. The algorithm used in this paper is competitive with respect to the one known in literature an approach based on the harmonic balance method operated in frequency domain.

Key words: electromechanical system, steady-state analysis, periodic solutions, analysis in time domain, discrete differential operator, iterative algorithms.

1. Introduction

Steady-state analysis belongs to the basic methods used in electrical engineering. The respective methods are essential tools for exploring the properties of electrical systems. Steady-states of electrical machines are of particular interest since they provide information on technical and economic parameters. Determining steady-state for AC machines is complicated because of the need to find stationary solutions for differential equations of the form:

$$\frac{\mathrm{d}}{\mathrm{d}t} = \left(\boldsymbol{\Psi}\left(\mathbf{i},\, \varphi\right)\right) + \mathbf{R}\mathbf{i} = \mathbf{u}(t), \tag{1a}$$

$$\mathrm{J}\frac{\mathrm{d}^2\varphi}{\mathrm{d}t^2} + \mathrm{D}\frac{\mathrm{d}\varphi}{\mathrm{d}t} = \frac{\partial E_{co}(\mathbf{i},\, \varphi)}{\partial \varphi} + T_m(t,\, \varphi), \tag{1b}$$

where: $\mathbf{i}$ is the vector of independent currents, φ the rotary angle, $\boldsymbol{\Psi}(\mathbf{i},\, \varphi)$ the vector of linked fluxes, $\mathbf{R}$ the resistance matrix, $\mathbf{u}(t)$ the vector of supply voltages, $E_{co}(\mathbf{i},\, \varphi)$ the magnetic co-energy function, J the moment of inertia, D the damping coefficient, and $T_m(t,\, \varphi)$ the mechanical load torque. Equation (1a) describes the electromagnetic relation in the machine, whereas (1b) covers the rotational motion [1–3]. Together, they constitute a set of nonlinear differential equations which cannot be solved directly analytically. There are two physical reasons for the nonlinearity: the saturation of the machine's magnetic circuit, expressed in nonlinear relations of linked fluxes versus currents and rotary angle; the electromechanical interactions as effects of the nonlinear co-energy function with respect to currents and rotary angle. Often, the electromagnetic and mechanical phenomena in the machine can be treated separately by assuming an angular velocity constant ($\varphi = \Omega t + \varphi_0$). For such cases, only equation (1a) should be considered, which is still nonlinear due to the magnetic saturation. In general, the steady-state solution can be predicted in form of a double Fourier series with two independent periods. The first one is related to the period of the supply voltages, and the second refers to the rotor's angular velocity that determines the period of inductance variations in time. However, in many cases, the problem of finding the steady-state solution can be facilitated by looking for a periodic time function.

There exist two groups of methods enabling a direct determination of periodic or double-periodic steady-state solutions for nonlinear dynamic systems. The first is the harmonic balance method which operates in the frequency domain using the Fourier series representation of all differential equation terms. The basic assumption is that solutions with known periods exist. The method leads to a set of algebraic equations that determine the Fourier series coefficients of the solutions. The approach is commonly used for linear and nonlinear electrical circuits [4–8], electrical machines [3, 9–13], and also is combined with finite element method for electromagnetic devices [14–19]. In [20–24] harmonic balance is used for steady-state analysis of devices with semiconductor switching elements. In cases of nonlinearity, the harmonic balance equations of the Fourier coefficients are nonlinear and can be solved iteratively. The method becomes complicated because it requires multiple calculations of nonlinear time functions that appear in the differential equations using the Fourier series of solutions and vice versa, calculations of the Fourier series coefficients of those new time functions. Hence, such iterative algorithms are rather complicated.

An alternate approach is to determine the steady-state curves directly in the time domain. This is the most commonly used

*e-mail: pesobczy@cyf-kr.edu.pl

Manuscript submitted 2017-10-02, initially accepted for publication 2018-01-16, published in October 2018.

approach in finite-difference methods, in which the derivatives are substituted by discrete finite-difference operators engaging the values at adjacent time points [25–27]. The difference equations for periodic steady-states are obtained by assuming that the values at the beginning of the period are equal to the values at the end. This approach is strictly limited to periodic solutions. The creation of difference equations is especially simple for differential equations written in the normal form. The difference equations of nonlinear systems are also nonlinear and can be solved by applying iterative procedures. The latter are less complicated because they operate directly in the time domain. There exist other methods reducing the problem to linear one [28, 29] or combining the numerical integration with boundary value problems, like the waveform relaxation method [30–33].

However, to identify the steady-states of nonlinear systems in engineering, the equations are solved numerically until the transient component vanishes and only the steady-state component remains. It seems to be not very effective due to the creation of unnecessary data and the application of advanced hardware and software. Therefore, specialized simple methods of steady-state analysis of nonlinear dynamic systems, analogous to such methods for linear systems, should be developed and the corresponding algorithms should be added to engineering software packages.

In [34–37], an alternate approach to determine the periodic steady-state solution for nonlinear electrical circuits has been proposed and tested. The method presented in [35–37] combines harmonic balance and direct time-domain methods. Based on harmonic balance relations between the periodic function and its first derivatives, the relation between the values of the function and its derivative for a set of time points is constituted in the form of a discrete differential operator. This operator determines the values of the first derivatives by engaging all values of the function for the same set of time points regarding one period. Using that operator, difference equations that determine steady-state solutions directly in the time domain for the electrical machine equations (1a, b) can be derived. In [38], it has been shown how to extend that approach onto double-periodic solutions, which is impossible for other time domain methods.

In [35], the mentioned novel approach has been successfully tested for equation (1a) for a simple electromechanical converter by assuming a periodic supply voltage, a linear magnetic circuit, and a constant angular velocity. In [37], the steady-state for the same converter has been studied assuming a nonlinear magnetic circuit. In this paper, the direct time-domain approach is tested for the same converter considering both equations (1a) and (1b), i.e. taking into account electromechanical interactions.

2. Formulation of difference equations of AC machines for periodic steady-states

The equations of AC machines can be obtained using the Lagrange formalism for electromechanical systems [1–3]. Equations (1a, b) are just examples. In general, equations of electromechanical systems are Lagrange equations which have the following form for systems under holonomic constraints:

$$\frac{\mathrm{d}}{\mathrm{d}t}\left(\frac{\partial L(\mathbf{x},\mathbf{v})}{\partial v_n}\right)-\frac{\partial L(\mathbf{x},\mathbf{v})}{\partial x_n}=f_n;\ \text{for}\ n=1,\ldots,N, \quad (2.1)$$

where $\mathbf{x}$ is the vector of the generalized electromechanical coordinates $(x_1, \ldots, x_N)$, $\mathbf{v}$ the vector of the generalized electromechanical velocities $(v_1, \ldots, v_N)$, $L(\mathbf{x}, \mathbf{v})$ the Lagrange function, and f_n the external electromechanical forces. The Lagrange equations are a set of ordinary second-order nonlinear differential equations which can be written for future consideration in the following general form:

$$\frac{\mathrm{d}^2}{\mathrm{d}t^2}\left(\mathbf{A}_2(\mathbf{x})\cdot\mathbf{x}\right)+\frac{\mathrm{d}}{\mathrm{d}t}\left(\mathbf{A}_1(\mathbf{x})\cdot\mathbf{x}\right)+\mathbf{A}_0\cdot\mathbf{x}=\mathbf{f}(t), \quad (2.2)$$

where $\mathbf{A}_0(\mathbf{x})$, $\mathbf{A}_1(\mathbf{x})$, and $\mathbf{A}_2(\mathbf{x})$ are matrices with nonlinear functions of the variables $(x_1, \ldots, x_N)$. If the steady-state solutions of these equations can be predicted as periodic time functions with a known period T, they can be directly quantitatively determined using discrete difference equations created on the base of the novel discrete differential operator described in [35, 36]. This operator relates values of the first derivative of a periodic function to values of the function itself for a set of time instants $\{t_r\}$, selected as follows:

$$t_k = k\cdot\Delta T \ \text{ for } -K\le k\le K, \ \text{ where } \ \Delta T = T/(2K+1).$$

Thus, time points are located in the interval $-T/2 \le t_k \le T/2$ at a distanceΔT. The relation has the form:

$$\mathbf{x}' = \mathbf{D}\cdot\mathbf{x}, \quad (2.3)$$

where $\mathbf{x}'$ is a hyper-vector containing the vectors $\mathbf{x}'_k$ of the first derivative for the selected set of time instants:

$$\mathbf{x} = \begin{bmatrix} x'_K & \cdots & x'_1 & x'_0 & x'_{-1} & \cdots & x'_{-K}\end{bmatrix}^T,$$

and $\mathbf{x}$ is a hyper-vector containing the vectors $\mathbf{x}_k$ of the function for the same set of time instants:

$$\mathbf{x} = \begin{bmatrix} x_K & \cdots & x_1 & x_0 & x_{-1} & \cdots & x_{-K}\end{bmatrix}^T,$$

The matrix $\mathbf{D}$ is a discrete differential operator for periodic functions:

$$\mathbf{D} = \begin{bmatrix} \mathbf{0} & -\mathbf{b}_1 & -\mathbf{b}_2 & \cdots & \cdots & \cdots & -\mathbf{b}_{2K} \\ \mathbf{b}_1 & \ddots & \ddots & \ddots & & & \vdots \\ \vdots & \ddots & \mathbf{0} & -\mathbf{b}_1 & -\mathbf{b}_2 & & \vdots \\ \mathbf{b}_K & \cdots & \mathbf{b}_1 & \mathbf{0} & -\mathbf{b}_1 & \cdots & -\mathbf{b}_K \\ \vdots & & \mathbf{b}_2 & \mathbf{b}_1 & \mathbf{0} & \ddots & \vdots \\ \vdots & & & \ddots & \ddots & \ddots & -\mathbf{b}_1 \\ \mathbf{b}_{2K} & \cdots & \cdots & \cdots & \mathbf{b}_2 & \mathbf{b}_1 & \mathbf{0} \end{bmatrix}.$$

It is composed of the diagonal matrices $\mathbf{b}_k$ with the dimension (N×N):

$$\mathbf{b}_k = \mathrm{diag}\left[\,\mathrm{b}_k \quad \cdots \quad \mathrm{b}_k \quad \cdots \quad \mathrm{b}_k\,\right].$$

having the elements b_k on the main diagonal:

$$\mathbf{b}_k = \frac{\Omega}{2\mathrm{K}+1} \cdot \sum_{l=1}^{\mathrm{K}} 2k \cdot \sin\left(k \cdot l \cdot \frac{2\pi}{2\mathrm{K}+1}\right). \tag{2.4}$$

The difference equations for (2.2) can be very easily obtained using the discrete differential operator $\mathbf{D}$:

$$\mathbf{D} \cdot \mathbf{D} \cdot \mathbf{A}_2(\mathbf{x}) \cdot \mathbf{x} + \mathbf{D} \cdot \mathbf{A}_1(\mathbf{x}) + \mathbf{A}_0(\mathbf{x}) \cdot \mathbf{x} = \mathbf{f}, \tag{2.5}$$

where $\mathbf{f}$ is a hyper vector containing the vectors $\mathbf{f}_k$ of the forced functions for the selected set of time instants:

$$\mathbf{f} = \left[\mathbf{x}_{\mathrm{K}} \quad \cdots \quad \mathbf{x}_1 \quad \mathbf{x}_0 \quad \mathbf{x}_{-1} \quad \cdots \quad \mathbf{x}_{-\mathrm{K}}\right]^T.$$

It is a set of nonlinear algebraic equations which can be solved numerically. The simple iterative method leads to:

$$\left(\mathbf{D}^2 \cdot \mathbf{A}_2(\mathbf{x}^i) + \mathbf{D} \cdot \mathbf{A}_1(\mathbf{x}^i) + \mathbf{A}_1(\mathbf{x}^i)\right) \cdot \mathbf{x}^{i+1} = \mathbf{f}, \tag{2.6}$$

Equation (2.6) provides the basis for an iterative algorithm to determine the periodic steady-state solution directly in time domain.

3. Application example to study steady-state electromechanical interactions

A simple single-phase electromechanical reluctance converter has been chosen as a representative for the difficulties in finding the steady-state performance considering electromechanical interactions. The converter is schematically shown in Fig. 1. The converter equations have the form:

$$\frac{\mathrm{d}\psi(i,\varphi)}{\mathrm{d}t} + \mathrm{R} \cdot i = u(t), \tag{3.1a}$$

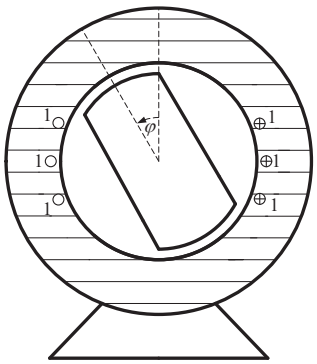

Fig. 1. Single-coil reluctance converter

$$\mathrm{J}\frac{\mathrm{d}^2\varphi}{\mathrm{d}t^2} + \mathrm{D}\frac{\mathrm{d}\varphi}{\mathrm{d}t} = T_{em}(i,\varphi) + T_m(t,\varphi), \tag{3.1b}$$

where i is the coil current, φ the rotary angle, $\psi(i,\varphi)$ the linked coil flux, R the coil resistance, $u(t)$ the supply voltage, J the moment of rotor inertia, D the mechanical damping factor, $T_m(t,\varphi)$ the mechanical torque, and $T_{em}(i,\varphi)$ the electromagnetic torque given by:

$$T_{em}(i,\varphi) = \frac{\partial}{\partial\varphi}\int_0^i \psi(i',\varphi)di'. \tag{3.2}$$

For exemplary computations, the equation for the coil linked flux is as follow:

$$\psi(i,\varphi) = L(i,\varphi) \cdot i, \tag{3.3}$$

where

$$L(i,\varphi) = L_0(i) + L_2(i) \cdot \cos 2\varphi + L_4(i) \cdot \cos 4\varphi, \tag{3.4}$$

with

$$L_0(i) = \mathrm{L}_0 + \mathrm{a}_{02} \cdot i^2 + \mathrm{a}_{04} \cdot i^4,$$
$$L_2(i) = \mathrm{L}_2 + \mathrm{a}_{22} \cdot i^2 + \mathrm{a}_{24} \cdot i^4,$$
$$L_4(i) = \mathrm{L}_4 + \mathrm{a}_{42} \cdot i^2 + \mathrm{a}_{44} \cdot i^4.$$

Equations (3.1a, b) take into account both the rotor reluctance and nonlinearity of the magnetic circuit.

By assuming:

- a mono-harmonic supply voltage
$$u(t) = \mathrm{U}_\mathrm{m} \cdot \cos(\Omega \cdot t),$$
- a constant load torque $T_m(t,\varphi) = \mathrm{T}_\mathrm{m}$,
- a synchronously running motor with an angular velocity Ω but with an angle perturbation $\Delta\varphi(t)$, i.e. $\varphi(t) = \Omega \cdot t + \Delta\varphi(t)$,

the steady-state solutions of the current $i(t)$ and the rotary angle perturbation $\Delta\varphi(t)$ can be encountered as periodic time functions:

$$i(t) = i(t+\mathrm{T}) \;\text{ and }\; \Delta\varphi(t) = \Delta\varphi(t+\mathrm{T}), \tag{3.5}$$

where $\mathrm{T} = 2\pi/\Omega$. Therefore, with the modified equations of $i(t)$ and $\Delta\varphi(t)$:

$$\frac{\mathrm{d}\psi(i,\Delta\varphi)}{\mathrm{d}t} + \mathrm{R} \cdot i = \mathrm{U}_\mathrm{m} \cdot \cos(\Omega \cdot t), \tag{3.6a}$$

$$\mathrm{J}\frac{\mathrm{d}^2\Delta\varphi}{\mathrm{d}t^2} + \mathrm{D}\frac{\mathrm{d}\Delta\varphi}{\mathrm{d}t} = T_{em}(i,\Delta\varphi) + T_m - \mathrm{D} \cdot \Omega, \tag{3.6b}$$

periodic steady-state solutions can be predicted. These equations should be written in the form of (2.2). However, in the nonlinear functions $\psi(i,\Delta\varphi)$ and $T_{em}(i,\Delta\varphi)$ appear the trigonometric terms $\cos\left(n \cdot (\Omega t + \Delta\varphi)\right)$ and $\sin\left(n \cdot (\Omega t + \Delta\varphi)\right)$ which should be presented in the form $a(i,\Delta\varphi,t) \cdot \Delta\varphi$. This can be done by defining two functions:

$$f_s(x) = \begin{cases} \dfrac{\sin x}{x} & \text{at } x \neq 0 \\ 1 & \text{at } x = 0, \end{cases}$$
$$f_c(x) = \begin{cases} \dfrac{1-\cos x}{x} & \text{at } x \neq 0 \\ 0 & \text{at } x = 0. \end{cases} \tag{3.7}$$

These functions are determined in the interval $-\pi/2 < x < \pi/2$ and they allow to obtain the relations:

$$\sin x = f_s(x) \cdot x, \qquad \cos x = 1 - f_c(x) \cdot x. \tag{3.8}$$

Useful relations for equations (3.6a, b) can be obtained by introducing $x = n \cdot (\Omega t + \Delta\varphi)$:

$$\cos\big(n \cdot (\Omega t + \Delta\varphi)\big) = \cos(n \cdot \Omega t) + -n \cdot \big(\sin(n \cdot \Omega t) \cdot \cdot f_s(n \cdot \Delta\varphi) + \cos(n \cdot \Omega t) \cdot f_c(n \cdot \Delta\varphi)\big) \cdot \Delta\varphi, \tag{3.9a}$$

$$\sin\big(n \cdot (\Omega t + \Delta\varphi)\big) = \sin(n \cdot \Omega t) + n \cdot \big(\cos(n \cdot \Omega t) \cdot \cdot f_s(n \cdot \Delta\varphi) + \sin(n \cdot \Omega t) \cdot f_c(n \cdot \Delta\varphi)\big) \cdot \Delta\varphi. \tag{3.9b}$$

The resulting equation, written in the form of (2.2), is as follow:

$$\frac{\mathrm{d}^2}{\mathrm{d}t^2}\begin{bmatrix} 0 & 0 \\ 0 & \mathrm{J} \end{bmatrix}\begin{bmatrix} i \\ \Delta\varphi \end{bmatrix} + \frac{\mathrm{d}}{\mathrm{d}t}\begin{bmatrix} a_{1,11}(i, \Delta\varphi, t) & a_{1,12}(i, \Delta\varphi, t) \\ 0 & \mathrm{D} \end{bmatrix}\begin{bmatrix} i \\ \Delta\varphi \end{bmatrix} + + \begin{bmatrix} \mathrm{R} & 0 \\ a_{0,21}(i, \Delta\varphi, t) & a_{0,22}(i, \Delta\varphi, t) \end{bmatrix}\begin{bmatrix} i \\ \Delta\varphi \end{bmatrix} = = \begin{bmatrix} \mathrm{U_m} \cdot \cos(\Omega \cdot t) \\ \mathrm{T_m} - \mathrm{D} \cdot \Omega \end{bmatrix}. \tag{3.10}$$

Functions $a_{1,11}(i, \Delta\varphi, t)$, $a_{1,21}(i, \Delta\varphi, t)$, $a_{0,21}(i, \Delta\varphi, t)$, and $a_{0,11}(i, \Delta\varphi, t)$ can be determined in detail based on (3.2), (3.3), (3.7), (3.8), and (3.9a, b). Equation (3.10) uniquely identifies the vector of solution $\mathbf{x}$, the matrices $\mathbf{A}_0(\mathbf{x})$, $\mathbf{A}_1(\mathbf{x})$, $\mathbf{A}_2(\mathbf{x})$, and the forced function vector $\mathbf{f}$ of the difference equation (2.2). It allows writing difference equations (2.5) for that case. The periodic steady-state solutions for $i(t)$ and $\Delta\varphi(t)$ can be found by solving the equation iteratively with respect to (2.6).

4. Results of numerical tests

The iterative algorithm described above has been implemented in the MATLAB package. In [37], the results of the above-described algorithms are presented for the case when equation (3.1a) of the converter is considered under the assumption that the rotary movement is uniquely determined, i.e. $\varphi(t) = \Omega \cdot t + \varphi_0$. The results confirm correctness and efficiency of the algorithm for nonlinear coil characteristics in comparison to results of simulations. The currents obtained from the computations have been used as starting data for solving (2.6) with the algorithm, additionally assuming that angle perturbations do not appear and $\Delta\varphi(t) = \varphi_0$. In [37], it has been mentioned that the result differences of linear and nonlinear coil characteristics are rather small. Thus, during the first attempt to study electromechanical interactions, magnetic linearity has been assumed by expressing the coil inductance as $L(\varphi) = \mathrm{L}_0 + \mathrm{L}_2 \cdot \cos 2\varphi + \mathrm{L}_4 \cdot \cos 4\varphi$. Calculations have been performed for the same data as in [37] (with unit values): $\mathrm{U_m} = 0.6$, $\Omega = 1.0$, $\mathrm{L}_0 = 0.625$, $\mathrm{L}_2 = 0.375$, $\mathrm{L}_4 = 0.050$, and $\mathrm{R} = 0.1$, adding $\mathrm{J} = 10.0$ and $\mathrm{D} = 0.01$. To find the angle φ_0, the mean value of the electromagnetic torque $\mathrm{T}_{\mathrm{em},0}$ versus φ_0 has been determined (shown in Fig. 2). Calculations have been performed considering $\mathrm{K} = 100$ and 201 time points over one period.

In Fig. 2, points are marked at which the load torque and the mean value of the electromechanical torque are balanced. For a load torque of $\mathrm{T_{em}} = \pm 0.03635$ (app. 0.5 $\mathrm{T_{em,\,max}}$), the corresponding angles are: $\varphi_1 = 1.4875$, $\varphi_2 = 0.498$, $\varphi_3 = 0.0255$, $\varphi_4 = 1.903$, and $\varphi_5 = -1.683$.

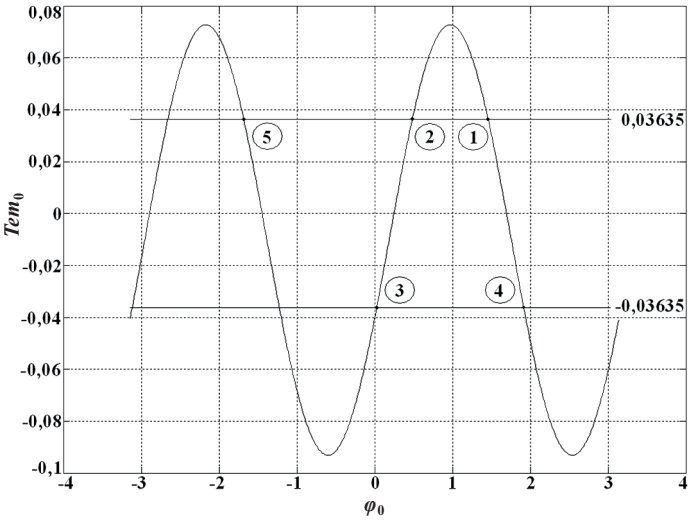

Fig. 2. Mean value of electromagnetic torque versus angle

It is commonly known that a stable static balance between the torques is possible when the first derivative of the curve in Fig. 2 is negative, i.e. the points φ_1, φ_4, and φ_5 are stable and the points φ_2 and φ_3 are unstable. The current curves at these five points have been calculated using the algorithm presented in [37] and are shown in Fig. 3 with respect to the voltage (black curve). Together with the angles φ_1, φ_2, φ_3, φ_4, and φ_5, they constitute the starting data for the algorithm considering equation (3.10). The numbers in Fig. 3 refer to the points in Fig. 2. The current curves for points '1' and '5' overlap. However, the algorithm finds only the solutions for the unstable part of the curve in Fig. 2, even if starting very closely to the stable points. The results of two exemplary tests are shown for φ_1 and φ_2 hereafter.

In Figs. 4a, b, the curves of the angle perturbation $\Delta\varphi(t)$ and the current $i(t)$ are shown as successive iterations starting at the unstable point '2', i.e. at $\varphi_2 = 0.498$. Fig. 4a shows how

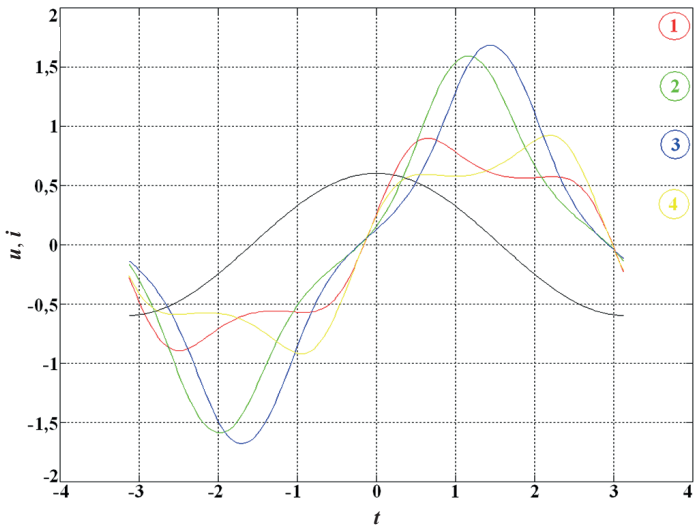

Fig. 3. Current curves for different angles φ_0

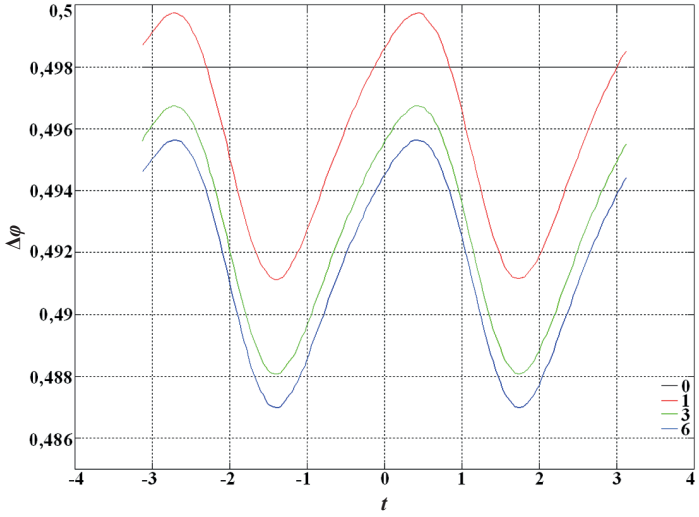

Fig. 4a. Curves of angle perturbation $\Delta\varphi(t)$ as successive iterations starting at φ_2

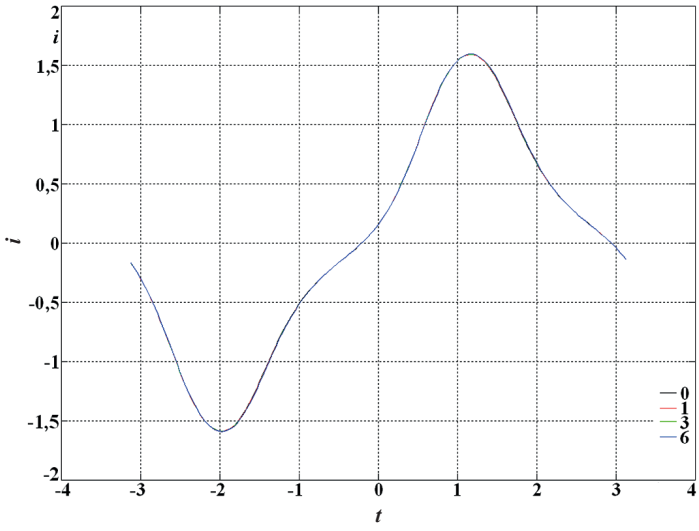

Fig. 4b. Current curves $i(t)$ as successive iterations starting at φ_2

the angle perturbation is changed, whereas Fig. 4b presents the current. In Fig. 4b, the curves nearly overlap. The steady-state solution is readily found after six iterations.

In Fig. 5, the curves of the current $i(t)$ and the angle perturbation $\Delta\varphi(t)$ are shown for chosen iterations (0, 3, 4, 5, 10, and 20) for starting at the stable point $\varphi_1 = 1.4875$. After 20 iterations, the algorithm reaches the same solution as in Figs. 4a, b at an unstable point close to $\varphi_2 = 0.498$. The iteration process is very dynamic and curves change significantly during iterations, which is illustrated in the figures below.

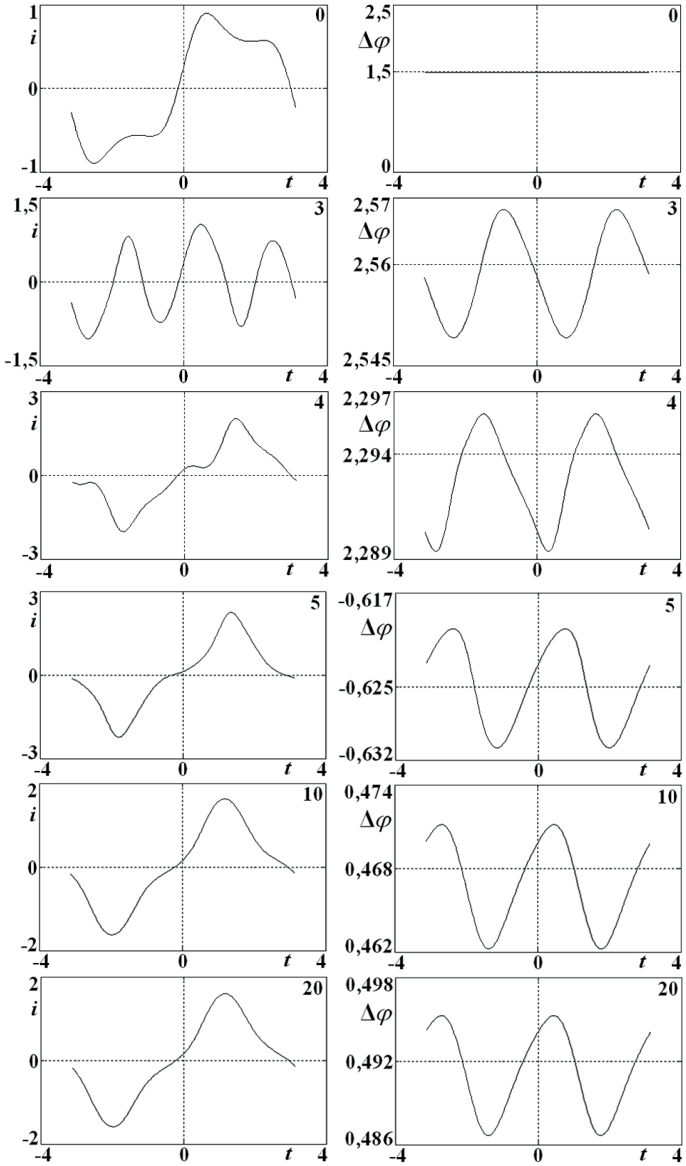

Fig. 5. Curves of current $i(t)$ and angle perturbation $\Delta\varphi(t)$ for chosen iterations starting at φ_1

Figure 6a presents the changes of the mean value of angle perturbation and Fig. 6b shows the changes of its magnitude during iterations. These are just exemplary results but such tendencies have also been observed for different starting points.

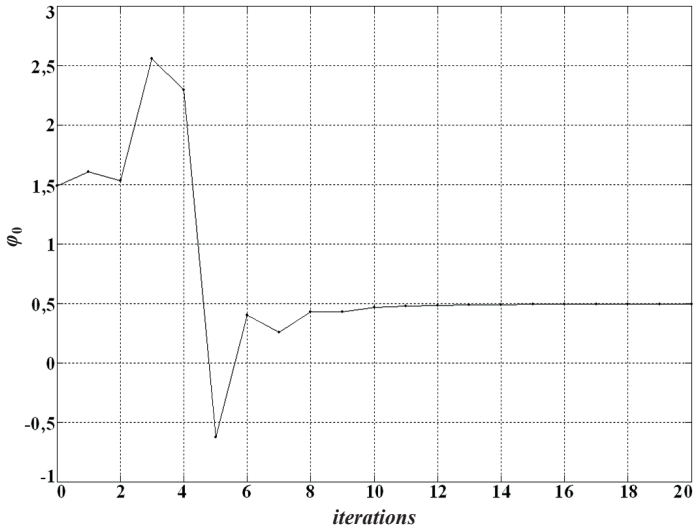

Fig. 6a. Mean value of angle perturbation $\Delta\varphi(t)$ as successive iterations starting at φ_1

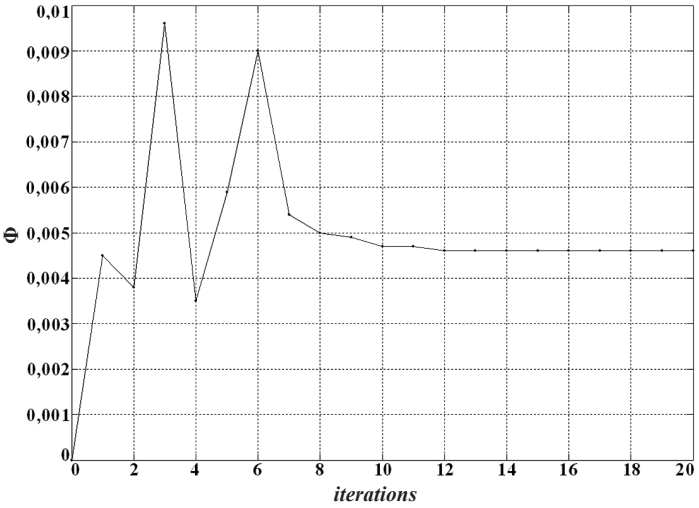

Fig. 6b. Magnitude of angle perturbation $\Delta\varphi(t)$ as successive iterations starting at φ_1

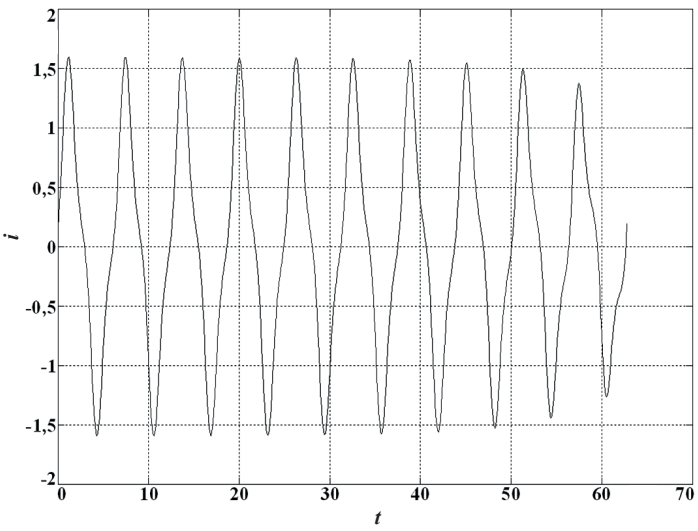

Fig. 7a. Current $i(t)$ in transient for starting at the unstable point '2'

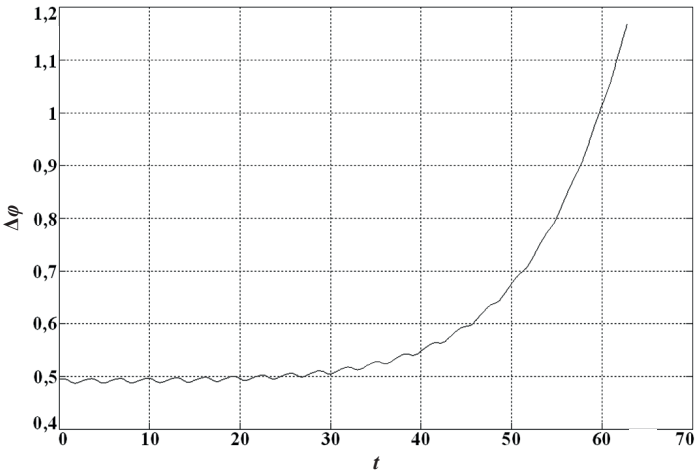

Fig. 7b. Angle perturbation $\Delta\varphi(t)$ in transient for starting at the unstable point '2'

The algorithm always finds the solution in the unstable part of the characteristic curve.

In order to explain that phenomenon, the differential equations (3.1a, b) have been solved numerically using the classical ode45 solver offered by MATLAB. The same data as in the algorithm have been applied. The initial conditions have been determined based on the starting data for the algorithm.

In Figs. 7a, b, the simulation results are shown for starting at the unstable point '2' of Fig. 2. The initial conditions for the numerical integration have been found based on the solutions, which are presented in Figs. 4a, b.

Evidently, the transient performance shows that the angle perturbation has added an exponential component to the periodic curve shown in Fig. 4b. The current exhibits at the beginning a periodic oscillation, as shown in Fig. 4a. This confirms that point '2' is unstable for static balance between electromechanical and mechanical torques. The algorithm finds a solution at this point because the curves of the current and angle perturbation are periodic at steady-state.

Figures 8a, b present the simulation results for starting at the stable point '1' of Fig. 2. For x case, the initial conditions have been determined based on the solutions obtained from the algorithm, assuming $\varphi(t) = \Omega \cdot t + \varphi_0$. The steady-state current curve is shown in Fig. 3. The transient performance shows that the angle perturbation is not periodic with the period of the supply voltage. However, it contains an additional periodic component with an unknown period at low frequencies. The current is also not periodic and it is modulated with a low frequency due to the angle perturbation while mostly retaining the curve form depicted in Fig. 3. However, the solution is stable but not periodic as it has been assumed for the algorithm for a direct steady-state analysis. This explains why the solution cannot be found by the algorithm. Slow angle perturbations depend strongly on the parameters in the mechanical equation.

In Fig. 9, the steady-state angle perturbations at the stable condition (point '1') are shown which are obtained by simula-

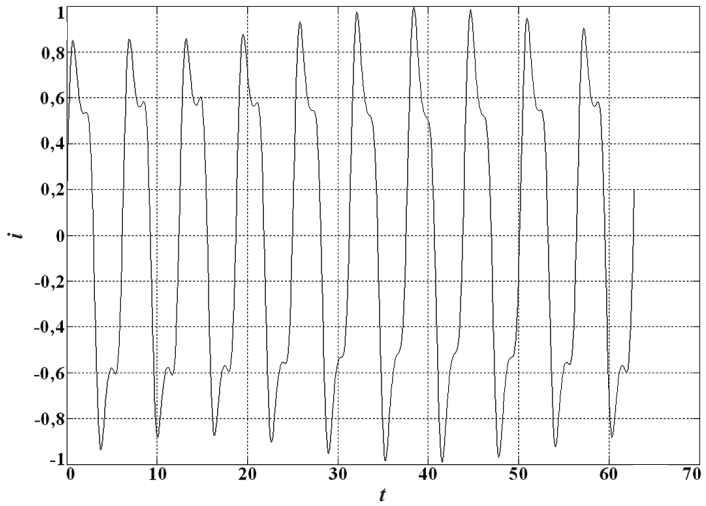

Fig. 8a. Current $i(t)$ in transient for starting at the stable point '1'

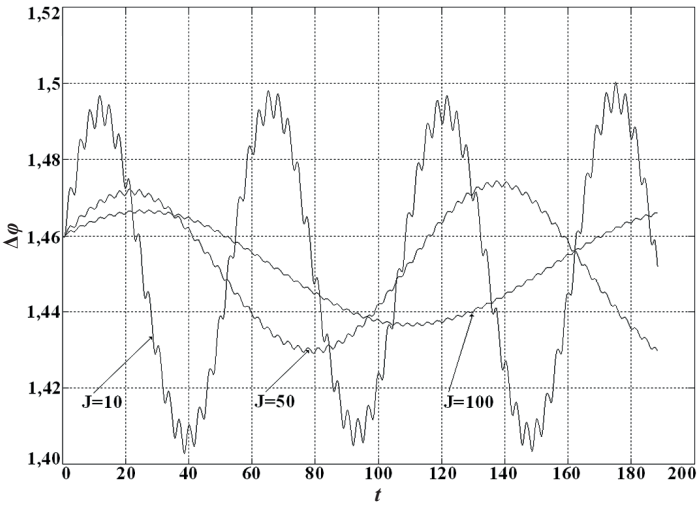

Fig. 9. Angle perturbation $\Delta\varphi(t)$ for different moments of inertia at the stable point '1' (simulation results)

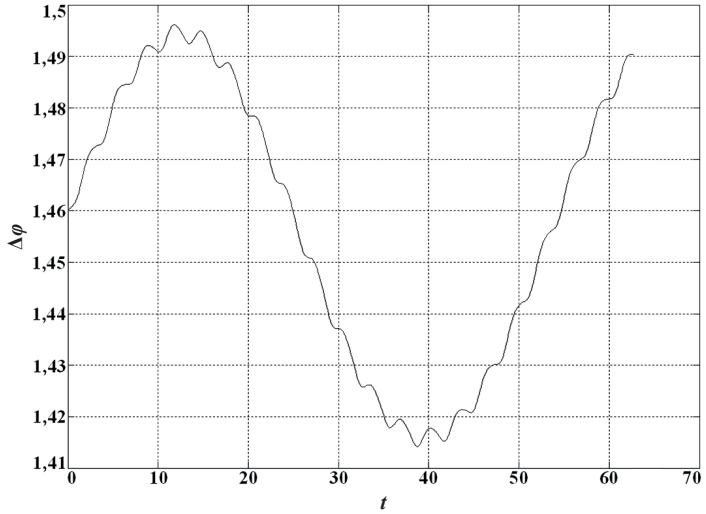

Fig. 8b. Angle perturbation $\Delta\varphi(t)$ in transient for starting at the stable point '1' (simulation results)

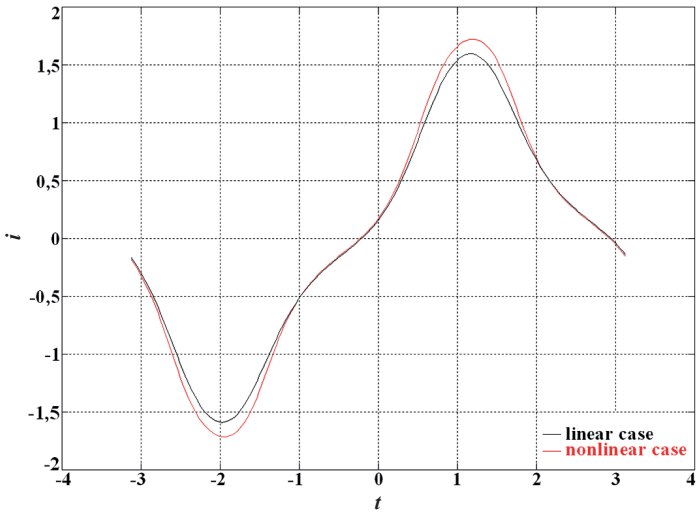

Fig. 10a. Influence of saturation on the current curve $i(t)$ at starting point '2'

tions for three different moments of inertia: J = 10, J = 50, and J = 100. The magnitudes of both components are related to the voltage frequency and the frequency of the angle perturbation decreases with an increasing moment of inertia (goes to zero for an infinite moment of inertia). However, the current keeps almost the same curve shape as for $\varphi(t) = \Omega \cdot t + \varphi_0$.

The above-described electromechanical phenomena do not change if a nonlinear converter's magnetic circuit is taken into account. The algorithm finds only the unstable points. The nonlinear coil characteristic of (3.3) has been calculated for the data in [37]:

$$L_0 = 0.625,\ a_{02} = -0.075,\ a_{04} = 0.00550,$$
$$L_2 = 0.375,\ a_{22} = -0.075,\ a_{24} = 0.00550,$$
$$L_4 = 0.050,\ a_{42} = -0.010,\ a_{44} = 0.00052.$$

Such a characteristic is valid for currents in the interval $|i(t)| < 2.0$. The calculation results of the steady-state curves at the starting point '2' of Fig. 2 are shown in Figs. 10a, b for the same rest

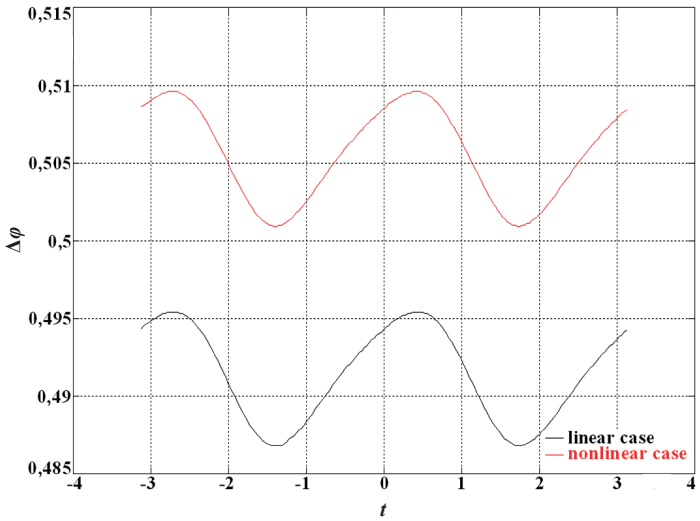

Fig. 10b. Influence of saturation on the angle perturbation curve $\Delta\varphi(t)$ at starting point '2'

data. Figure. 10a shows the current curves for a linear and nonlinear coil characteristic. Fig. 10b presents the corresponding angle perturbation curves. It is evident that the magnetic nonlinearity does not essentially change these curves.

The numerical test results show application difficulties regarding the study of electromechanical interactions. In fact, the algorithm finds a non-practical steady-state solution which is unstable. Further, the algorithm cannot find a stable solution. Nonetheless, the proposed algorithm has an important positive feature. It can find any existing periodic solution even if the algorithm starts very far from the solution.

5. Conclusions

This paper presents a new algorithm for the calculation of periodic steady-state solutions in the time domain for electrical machines. The algorithm comprises a nonlinear magnetic circuit and structural nonlinearity via the equation of motion. Further, the algorithm eliminates the necessity of Fourier series, which is necessary for the frequency domain approach. The key element of the proposed algorithm is a novel discrete differential operator. Numerical tests show the algorithm' disadvantages which can be achieved while determining steady-state electromechanical interactions.

Acknowledgements. This research has been carried on in the frame of project E-2/581/2016/DS founded by The Polish Ministry of Science and Higher Education.

References

[1] D.C. With and H.H. Woodson, *Electromechanical energy conversion*, J. Wiley &Sons, New York, (1959).
[2] A. Puchała, *Dynamics of electrical machines and electro- mechanical systems,* PWN, Warsaw, 1977, [in Polish],
[3] T.J. Sobczyk, *Methodological aspects of mathematical modelling of induction machines*, WNT, Warsaw, (2004), [in Polish].
[4] L.O. Chua and A. Ushida, „Algorithms for computing almost periodic steady-state response of nonlinear systems to multiple input frequencies", *IEEE Trans. Circuits and Systems*, vol. 28, 953–971, (1981).
[5] T.J. Sobczyk, "A reinterpretation of the Floquet solution of the ordinary differential equation system with periodic coefficients as a problem of infinite matrix", *Compel*, vol.5, 1–22, (1986).
[6] S. Yamada, K. Beshho, and J. Lu, "Harmonic balance finite element method application for nonlinear magnetic analysis", *IEEE Trans. Magn*etics, vol.25, 2971–2973, (1989).
[7] A. Semlyen, E. Acha, and H.W. Dommel, "Newton-type algorithms for the harmonic phasor analysis of nonlinear power circuits in periodical steady state with special reference to magnetic nonlinearities", *IEEE Trans. Power Delivery*, vol. 6, 1090–1098, (1991).
[8] T.J. Sobczyk, "Direct determination of two-periodic solution for nonlinear dynamic systems", *Compel*, Vol.13, 509–529, (1994).
[9] J. Rusek, *Computer analysis of induction machines by using the harmonic balance method*, Univ. of Mining & Metallurgy, Cracow, (2000), [in Polish].
[10] K. Weinreb, "Diagnostics of an induction-motor rotor by the spectral analysis of stator currents", *Thermal Engineering*, vol. 60, 1006–1023, (2013).
[11] T. Węgiel, *Space harmonic interactions in permanent magnet generators*, Pub. Cracow Univ. of Tech., Cracow, (2013).
[12] M. Radzik, *Algorithm for direct determination of stead-states in synchronous machines accounting for the equation of motion*, PhD Thesis, Cracow Univ. of Technology, (2011) [in Polish].
[13] Y. Takahashi, T. Kameari, and T. Tokumasu, "Convergence acceleration in steady state analysis of synchronous machines using time-periodic explicit error correction method", IEEE Trans. Magnetics, vol. 47/5, 1422–1425, (2011).
[14] S. Yamada and K. Bessho, "Harmonic filed calculation by the combination of finite element analysis and harmonic balance method", *IEEE Trans. Magnetics*, vol. 24/6, 2588–2590, (1988).
[15] S. Yamada, K. Beshho, and J. Lu, "Harmonic balance finite element method application for nonlinear magnetic analysis", *IEEE Trans. Magn*etics, vol.25, 2971–2973, (1989).
[16] J. Gyselinck, P. Dular, C. Geuzaine, and W. Legros, "Harmonic-balance finite element modeling of electromagnetic devices: a novel approach, *IEEE Trans Magnetics.*, vol. 38/2, 521–524, (2002).
[17] O. Deblecker and J. Lobry, "A new efficient technique for harmonic balance-finite element analysis of saturated electromagnetic devices", *IEEE Trans. Magnetics*, vol. 38, 535–538, (2006).
[18] X. Zhao, J. Lu, L. Li, Z. Cheng, and T. Lu, "Analysis of the DC bias phenomenon by the harmonic balance finite-element method, *IEEE Trans. Power Delivery*, vol. 26/1, 475–485, (2011).
[19] X. Zhao, J. Lu, L. Li, Z. Cheng, and T. Lu, "Analysis of the saturated electromagnetic devices under CD bias condition by the decomposed harmonic balance method", *COMPEL*, vol. 3/2, 498–513, (2012).
[20] T. Sobczyk and B. Sapiński, "Harmonic analysis of currents in R,L-systems with semiconductor switching devices", *COMPEL*, vol.3, 151–165, (1983).
[21] T. Sobczyk and B. Sapiński, "Analysis of phase controlled converters for induction motors", *IEEE Trans. Power Electronics*, vol.5, 172–181, (1990).
[22] J. Lu, S. Yamada, and H.B. Harrison, "Application of harmonic balance finite element method in the design of switching power supplies", *IEEE Trans. Ind. Electronics,* vol. 11/2, 347–355, (1996).
[23] L.T.G. Lima, A. Semleyn, and R. Irvani, "Harmonic domain periodic steady state modeling of power electronics apparatus: SVC and TCSC, *IEEE Trans, Power Delivery*, vol. 18, 960–967, (2003).
[24] D. Borkowski, *"Matrix converter as power flow controller in transmission line-operatio: analysis in frequency domain",* Monograph No. 428, Cracow University of Technology, (2013).
[25] R.D. Richtmayer and K.W. Morton, Difference methods for initial-value problems, J Willey & Sons, New York, (1967).
[26] R.L. Burden and J.D. Faires, *Numerical analysis*, 3rd ed., PWS-Kent Pub., Boston, (1985).
[27] Z. Fortuna, B. Macukow, and J. Wąsowski, *Numerical methods*, 7th ed., WNT, Warsaw, (2009). [in Polish]
[28] S. Herdem and M. Koksal, "A fangielskaast algorithm to compute the steady-state solution of nonlinear circuits by piecewise linearization", *Computers and Elec. Eng.* vol. 28, 91–101, (2002).

[29] A.J. Jordan, "Linearization of non-linear state equation", *Bull. Pol. Ac.: Tech.*, vol. 54/1, 63–73, (2006).

[30] O. Biro and K. Preis, "An efficient time domain method for non-linear periodic eddy current problems", *IEEE Trans. Magnetics*, vol. 42/4, 695–698, (2006).

[31] E. Lelarasmee, A.E. Ruchli, and A. Sangiovanni-Vincentelli, "The waveform relaxation method for time-domain analysis of large scale integrated circuits", *IEEE Trans. CADIC*, vol. 1/3, 131–145, (1982).

[32] G. Caron, T. Henneron, F. Piriou, and J-C Mipo, "Time-periodic condition of nonlinear magnetostatic problem coupled with electric circuit imposed by waveform relaxation method", *IEEE Trans. Magnetics*, vol. 52/3, (2016).

[33] G. Caron, T. Henneron, F. Piriou, and J-C Mipo, "Waveform relaxation-Newton method to determine steady state operation: application to three-phase transformer, *COMPEL*, vol. 37/3, 729–740, (2017).

[34] N. Garcia, „Periodic steady-state solutions of nonlinear circuits based on a differentiation matrix", *Proc. of 2010 IEEE Int.l Symp. Circuits and Systems,* 141–144, (2010).

[35] T.J. Sobczyk and M. Radzik, "Direct determination of periodic solution in time domain for electromechanical converters, *Tech. Trans.–Elec. Eng.*, Cracow Univ. of Tech., vol. 112/ 2-E, 73–82, (2015).

[36] T.J. Sobczyk and M. Radzik, "A new approach to steady state analysis of nonlinear electrical circuits", *COMPEL,* Emerald Pub. Ltd., vol.37/3, 716–728, (2017).

[37] M. Radzik and T.J. Sobczyk, "An algorithm of time domain steady-state analysis for electrical machines accounting for saturation", *Proc. of Symp. on El. Mach.* (SME 2017), IEEE Explore, Paper 13, (2017).

[38] T.J. Sobczyk, "Algorithm for determining two-periodic steady-states in AC machines directly in time domain", *Arch. of El. Eng., of Polish Academy of Science*, vol. 65/3, 575–583, (2016).